

See discussions, stats, and author profiles for this publication at: <https://www.researchgate.net/publication/258263462>

Combining GPS and GLONASS in all-in-view for time transfer

Article in Metrologia · May 2013
DOI: 10.1088/0026-1394/50/3/277

CITATIONS
12

READS
206

3 authors:



A. Harmegnies
Bureau International des Poids et Mesures
12 PUBLICATIONS 88 CITATIONS

SEE PROFILE



P. Defraigne
Royal Observatory of Belgium
145 PUBLICATIONS 1,742 CITATIONS

SEE PROFILE



Gérard Petit
Bureau International des Poids et Mesures
177 PUBLICATIONS 2,068 CITATIONS

SEE PROFILE

Some of the authors of this publication are also working on these related projects:



DEMETRA Horizon 2020 [View project](#)



Spacetime Metrology and Relativistic Geodesy [View project](#)

Combining GPS and GLONASS in all-in-view for time transfer

Aurélien Harmegnies¹, Pascale Defraigne² and Gérard Petit¹

¹ Bureau International des Poids et Mesures, Pavillon de Breteuil, 92312 Sèvres, France

² Royal Observatory of Belgium, Avenue Circulaire, 3, B-1180 Brussels, Belgium

E-mail: p.defraigne@oma.be, aharmeg@bipm.org and gpetit@bipm.org

Received 18 March 2013, in final form 23 April 2013

Published 31 May 2013

Online at stacks.iop.org/Met/50/277

Abstract

GPS code measurements have been used for three decades for remote clock comparison, also called Time Transfer. Initially based on a technique using common-view (CV) single-frequency measurements, GPS time transfer now mostly uses dual-frequency measurements from geodetic receivers processed in all-in-view (AV). With the completion of the GLONASS constellation, it has been possible to readily use it in the CV single-frequency mode, providing results similar to GPS for short-distance time links. However GLONASS results are not readily equivalent to GPS in the dual-frequency AV mode, necessary for any moderate- to long-distance link, and this paper shows how to achieve this. We first present the GLONASS upgrade of the R2CGGTTS software, a tool to provide dual-frequency measurements in a format dedicated to time transfer named CGGTTS (Common GPS GLONASS Time Transfer Standard). The GLONASS navigation files are used to determine satellite clocks and positions, and dual-frequency pseudorange measurements are linearly combined to compute the CGGTTS results in a similar way as for GPS. In a second part, we present the combination of GPS and GLONASS into one unique time transfer solution based on AV. The results are first corrected using precise satellite orbit and clock products delivered by the IGS analysis centre ESOC, and characterized by the same reference for the GPS and GLONASS satellite clocks. Then, the need to introduce satellite-dependent hardware delays in GLONASS results is emphasized, and a procedure is proposed for their determination. The time transfer solutions obtained for GPS-only and GPS+GLONASS are then compared. The combination of GPS and GLONASS results in AV provides a time transfer solution having the same quality as GPS only. Furthermore, comparisons show that even when increasing the number of observations in CV thanks to the combination of the two constellations, the AV remains superior to the CV solution in terms of noise and short term stability, especially for long baselines.

(Some figures may appear in colour only in the online journal)

1. Introduction

Measurements from Global Navigation Satellite Systems (GNSS) have been used since the 1980s [1] to perform precise and accurate time and frequency transfer (TFT). In its classical version, the GNSS time transfer is performed using clock offsets collected in a fixed format, called CGGTTS (Common GPS GLONASS Time Transfer Standard), as described in [2, 3]. These clock offsets represent the differences between the ground clock (UTC(k)) in most cases and the

reference timescale of the GNSS. They are obtained from the pseudorange measurements, corrected for the signal travel time (satellite–station), for the troposphere and ionosphere delays, and for the relativistic effects. A smoothing is then performed over 13 min observation tracks. Starting with C/A code receivers, the method was then upgraded to take advantage of the dual-frequency receivers measuring codes on both frequencies, which allows one to remove the ionosphere delays at the first order (i.e. 99.9% of the effect), thanks to the ionosphere-free dual-frequency combination. This

Table 1. Receivers used in the study. Columns 6 to 9 correspond to the GLONASS code availability in the RINEX files. Ref.Type column expresses the type of frequency standard used; information has been extracted from the *BIPM Annual Report on Time Activities* [12] and IGS website.

Receiver	Laboratory	Type of receiver	Location	Period	P1	P2	C1	C2	Ref.Type
AO.4	AOS	TTS-3/4	Poland	55927–55957	x	x	x	x	H-maser
BP1B	BIPM	TTS-3/4	France	55927–55953	x	x	x	x	Caesium
IP02	IPQ	TTS-3/4	Portugal	55927–55957	x	x	x	x	Caesium
BP1C	BIPM	PolaRx3eTR	France	55927–55957		x	x		Caesium
BRUX	ORB	PolaRx3eTR	Belgium	55927–55957		x	x		H-maser
VN3P	VMI	PolaRx3eTR	Vietnam	55927–55957		x	x		Caesium
SYDN	NMIA	JPS E.GGD	Australia	55927–55957	x	x	x		Caesium
ONSA	ONSALA	JPS E.GGD	Sweden	55944–55957	x	x	x		H-maser
SPT0	SP	JAVAD TRE.G3TH DELTA	Sweden	55944–55957	x	x	x		H-maser

led to a factor of two improvement in the stability of the intercontinental time links up to averaging times of 10 days (e.g. [4]).

As at the beginning, GNSS data were collected from one-channel receivers, the initial approach for time transfer was based on common view (CV hereafter) [1], i.e. the clock comparison was obtained from the differences between the CCGTTS results collected in both stations for each satellite track. When multi-channel receivers started to be used, the CV was adapted accordingly, and the clock comparison was computed as a weighted average of the differences between the CCGTTS results obtained in both stations for each satellite separately. The weight in that case was a function of the elevation since low elevation observations are more affected by noise and multipath. In order to improve the long-distance clock comparisons, it was proposed for multi-channel time links to replace the CV approach by the all-in-view (AV hereafter) approach [5], the success of which is made possible by the availability of precise satellite ephemerides and clock products, e.g. from the IGS. AV consists in computing separately for each station the weighted average of the CCGTTS results ('Av.REFGPS'), and thereafter computing the time link as the difference between the solutions obtained in the two stations.

Some timing receivers directly provide the CCGTTS results, but in order to be able to use classical geodetic receivers driven by an external clock for the time transfer applications with the same standards, dedicated software named R2CGGTTS was produced to compute the CCGTTS files from the raw observation data provided by the receivers in the RINEX format [6]. This software is currently used by a large portion of the time laboratories for their participation in TAI, through the technique TAIP3 [7]. Thanks to the growing constellation of GLONASS, some timing laboratories have now upgraded their equipment with receivers capable of observing both GPS and GLONASS. In the frame of improving robustness and stability of time links used in TAI, the BIPM started to use several time links based on GLONASS measurements in the computation of TAI [8]. These links are realized using CCGTTS results obtained from the C/A code measurements corrected for the ionospheric delays using IGS maps for total electron content (TEC) [9]. Currently, the GLONASS links used for TAI are computed in CV and this solution is then averaged with the GPS link computed in AV based on the L1C code. This, however, limits the

use of GLONASS to short baselines as the ionosphere is not completely corrected by the use of ionospheric maps. We propose here another approach which consists in using the ionosphere-free combination P3 and in combining the GPS and GLONASS measurements in one unique AV solution.

In view of the growing number of receivers suited to both GPS and GLONASS, we adapted the R2CGGTTS software to the use of GLONASS observations. Section 2 of this paper presents the adaptation of the software to process both GPS and GLONASS measurements from the same RINEX observation file. A major difference between the GLONASS and GPS constellations is that each GLONASS satellite transmits on a different frequency using a 15-channel frequency division multiple access (FDMA) technique. As a consequence, the signal delay in the receiver is different for each satellite group emitting a given frequency. This affects the code measurements, with differential biases up to 25 ns, as already shown by several authors [10, 11]. These differential biases must be either determined by calibration or estimated in addition to the clock solution. The satellite-dependent biases of the CCGTTS results are discussed in section 3. Finally, a last section presents the comparison between the time transfer solutions obtained from either GPS only or GPS+GLONASS observations.

To perform this study, RINEX data from various receivers suited to both GPS and GLONASS have been processed; the stations used are presented in table 1.

2. CCGTTS for GLONASS observation

The CCGTTS files contain the clock offsets between UTC(*k*) and the reference time scale of the GNSS, as realized by each satellite for conventional 13 min tracks appearing in the international BIPM tracking schedules. To make the distinction between GPS and GLONASS satellites in the CCGTTS version 2 format, GLONASS prn are incremented by 100 and will thus appear as three-digit numbers in this paper. In what follows, clock solutions from CCGTTS concerning GPS will be called 'REFGPS' and those concerning GLONASS will be reported as 'REFGLN'; when both constellation are concerned, the clock solutions from CCGTTS are called 'REFSYS'. These clock solutions are computed from the pseudorange measurements, corrected for the signal travel time (satellite–station) based on broadcast satellite orbits, for the troposphere and ionosphere delays, and for the relativistic

effects. The final results provided are the midpoint of a linear fit performed over 13 min observation tracks for each visible satellite. The pseudorange measurements can be either the code on $L1$ (P1 or C/A or C1) or $L2$ (P2 or C2 also named L2C), in which case the ionosphere delay must be further removed. It can also be the ionosphere-free combination of them named P3. As this combination removes completely the first order ionospheric error, it is preferably used when dual-frequency measurements are available. The R2CGGTTS software is therefore based on P3. The choice of the codes used for this combination is made upon the available observations at the first epoch of the RINEX files: for each frequency and for each constellation, the code having the greatest occurrence is chosen. In the case of equality between P1 and C1, or P2 and C2, then the P code is preferred for both GPS and GLONASS. Because P2C2 biases are not available, no correction is applied by the software; however, these biases are included in the inter-frequency bias (IFB) determination and are thus removed in combined GPS+GLONASS AV. For the same reason, in the R2CGGTTS upgrade presented here, the timing group delay (TGD) [13] used for GPS to get the measured ionosphere is not considered yet in GLONASS treatment.

2.1. Broadcast navigation data

Classically, the CGGTTS results are computed using the broadcast navigation signals for the satellite ephemerides and clocks. While GPS navigation messages provide parameters of keplerian orbits in WGS84 (very close to the International Terrestrial Reference Frame ITRF) every 2 h, the broadcast navigation message of the GLONASS constellation is given as a set of positions and velocities in the PZ-90 Earth-fixed system at a sampling rate of 30 min. As we are computing the CGGTTS from RINEX data in a post-processing, we have the choice between computing the GLONASS satellite positions either by numerical integration or by polynomial interpolation. Some comparison of these two computation approaches was presented in [14], and as the noise of the results was larger with the polynomial interpolation, we decided to implement the Runge–Kutta integration in the R2CGGTTS software.

2.2. Reference system

GLONASS broadcast orbits are expressed in the PZ-90 reference system, while station coordinates are in ITRF. Since 20 September 2007, PZ-90 has been aligned to ITRF2000 with an uncertainty of some centimetres according to the ICG 2007 recommendation [15]. Therefore, no reference system conversion has to be applied when using GLONASS broadcast navigation orbits since October 2007.

2.3. Time scale

Furthermore, a time correction must be introduced because the observation files from geodetic receivers providing both GPS and GLONASS are dated in GPS time, while the reference of the GLONASS broadcast navigation message is GLONASS time, which is aligned on UTC. The two time scales GPS and GLONASS therefore differ by an integer number of leap

seconds (N_{leap}), the same as between GPS time and UTC (note that this information is available in BIPM *Circular T* and announced by IERS in *Bulletin C*). This correction must thus be applied to convert the GLONASS ephemerides to GPS time:

$$\text{GPS time} = \text{GLONASS time} + N_{\text{leap}}. \quad (1)$$

2.4. CV or AV

As explained before, the results appearing in the CGGTTS files correspond to the differences between $\text{UTC}(k)$ and the reference of the broadcast satellite clocks. This reference is GPS time for GPS satellites and GLONASS time for the GLONASS satellites. In order to mitigate the errors due to the low precision of the broadcast satellite clocks and positions in CGGTTS results, the BIPM first correct the CGGTTS results using more precise satellite orbits and clock data before computing the time links for the computation of TAI. In this procedure, the BIPM uses the rapid version of the satellite orbits and clock products delivered by the International GNSS Service (IGS) for GPS satellites, and IAC (Information Analytical Centre) products for GLONASS results. Note that the GLONASS time links currently included in the computation of TAI are based on CV and C/A code observations [16]. The solutions obtained from GLONASS CV and from GPS AV are then averaged. In this study, a different way is chosen: the GLONASS and GPS results obtained with the ionosphere-free combination P3, will be used together in a combined AV solution. For this, it is necessary that both GPS and GLONASS results are given with respect to the same reference. The reference for the IAC satellite clock products is GLONASS time, and the reference for the IGR products is the rapid version of the IGS time scale (IGRT). As none of these products provide clock corrections for satellites of the two constellations, they cannot be used for the corrections of the CGGTTS results if these latter must be combined in AV. We therefore used the products delivered by one IGS analysis centre, ESOC, which provides satellite clocks for GPS as well as GLONASS satellites with the same reference for both constellations. Thanks to that, it is possible to compute an AV solution combining the CGGTTS results for satellites from both constellations. Clock solutions REFSYS using the GPS and GLONASS data from the BIPM receiver (BP1B) are reported in figure 1(a) with broadcast orbits and clocks and (b) with final ESOC clocks and precise orbits.

A first observation in figure 1(a) is the ~ 400 ns offset between REFGPS and REFGLN, which is mainly due to the difference between the GPS time and GLONASS time. This offset remains when correcting the REFSYS with the ESOC satellite clock products, because these products are aligned on the broadcast clocks, although GPS and GLONASS satellite clocks are given with respect to the same reference (ref). For a given receiver (rec), the relationship between the clock solution obtained from a GPS or a GLONASS satellite using the ESOC clock products is

$$(T_{\text{rec}} - T_{\text{ref}})_{\text{GPS}_{\text{sat}}} = (T_{\text{rec}} - T_{\text{ref}})_{\text{GLONASS}_{\text{sat}}} + B_{\text{rec}}^{\text{GLONASS}_{\text{sat}}}, \quad (2)$$

where $B_{\text{rec}}^{\text{GLONASS}_{\text{sat}}}$ is a daily bias for the satellite–receiver pair and has a magnitude around 400 ns.

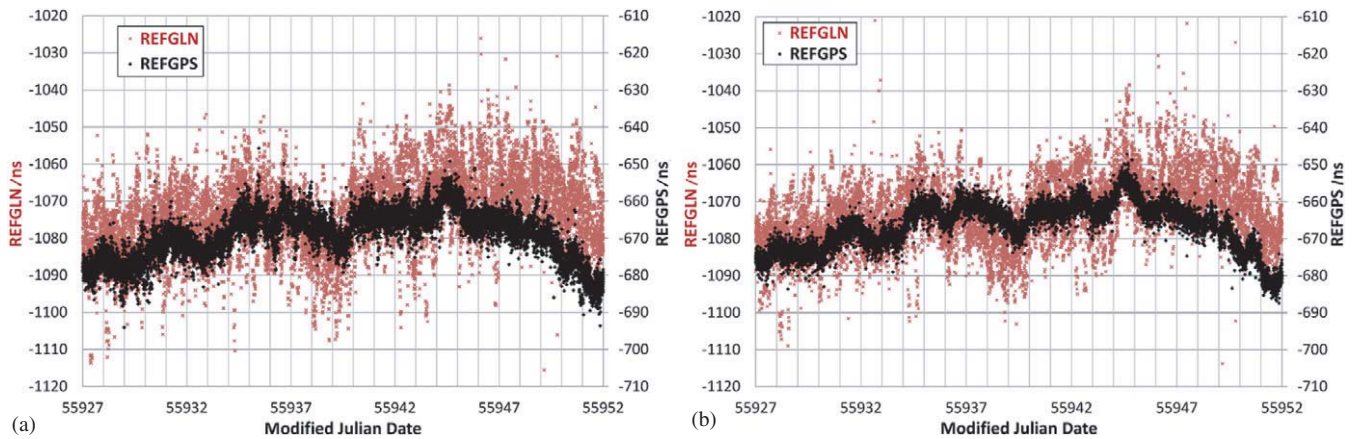


Figure 1. BP1B receiver CCGTTS clock solutions for GPS (REFGPS) and GLONASS (REFGLN).

As these biases are satellite-dependent, they are the cause of the higher dispersion of REFGLN data than of REFGPS data as observed in figure 2(b). As a consequence, these biases should be removed before combining GLONASS data and GPS data to get a calibrated time link. Two possible solutions exist: one is to directly calibrate the receiver for GLONASS signals; the alternative is to compute the satellite-dependent biases between the GPS solution and GLONASS signals and to remove these biases from the GLONASS data to get calibrated GLONASS results. These IFB are discussed in the next section as well as the procedure we propose to mitigate them.

3. Estimation of GLONASS IFBs

3.1. Origin of IFBs

As explained in the introduction, each satellite transmits on a different frequency using a 14-channel frequency division multiple access technique spanning either side of 1602.0 MHz known as the $L1$ band and either side of 1246.0 MHz known as the $L2$ band:

$$\begin{aligned} L1 &= 1602 \text{ MHz} + (n \times 0.5625) \text{ MHz}, \\ L2 &= 1246 \text{ MHz} + (n \times 0.4375) \text{ MHz}, \end{aligned} \quad (3)$$

where n is the frequency channel value ($n = -7, -6, -5, \dots, 0, \dots, 6$). Note that for each satellite, the ratio $L2/L1$ is always equal to $7/9$ as for GPS, so that the coefficients for P1 (or C1) and P2 (or C2) in the ionosphere-free combination, which depend on the ratio between the squared frequencies, are the same as those used for GPS.

Due to the frequency-dependent nature of the hardware delays in the receiver and in the antenna, these are different for each GLONASS frequency channel, inducing IFBs in the CCGTTS data as already mentioned in the previous section by the presence of $B_{\text{rec}}^{\text{GLONASS, sat}}$ in equation (2). An example of IFBs is visible in figure 2, which presents the REFGLN values for each satellite separately during one day. Not all the satellites were drawn in order to improve the visibility. The biases appear clearly between the solutions provided by the different satellites. IFBs can reach about 25 ns so that their effect is not negligible and is responsible for the noise of GLONASS data observed in figure 1. These IFB in the

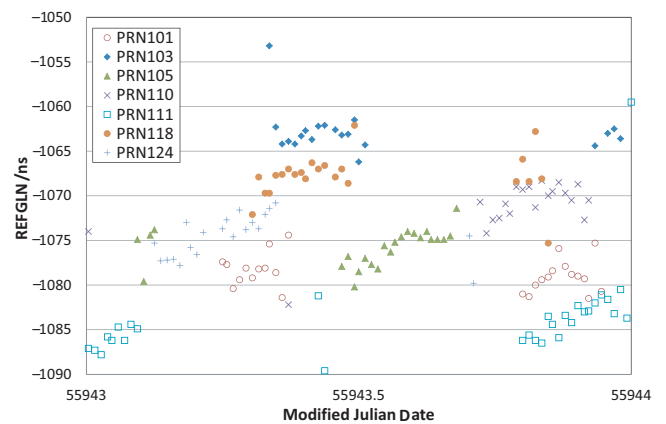


Figure 2. BP1B REFGLN corrected with ESOC precise orbits and clocks, sorted by satellite.

CGGTTS data must be removed before these data can be used in either CV or AV. Note that these biases are not removed in the procedure currently used by the BIPM for the computation of TAI. This results from the fact that for the two links presented in [16] an attempt to correct the REFSYS values for IFBs did not improve the final CV results. The biases for the code C/A are smaller than those for the ionosphere-free combination P3. The coefficients for the ionosphere-free combination are indeed 2.545 for P1 and 1.545 for P2, producing a possible amplification of the bias in P3 in comparison with the bias of C/A or P1. It will be shown here below that using P3 the correction for IFBs provides a significant improvement so that they cannot be neglected. As most of the receivers have not been calibrated for each of the GLONASS frequencies, the biases must be determined directly from the CCGTTS data. It was chosen to determine, for each receiver, the IFB of each GLONASS satellite with respect to the GPS AV solution, once REFSYS values from CCGTTS are corrected with precise ephemeris and clock products (from ESOC), according to the standard procedure used for BIPM TAI calculation.

3.2. ESOC clock stability

As described previously in section 2, REFSYS values are corrected with ESOC precise ephemerides and satellite clock

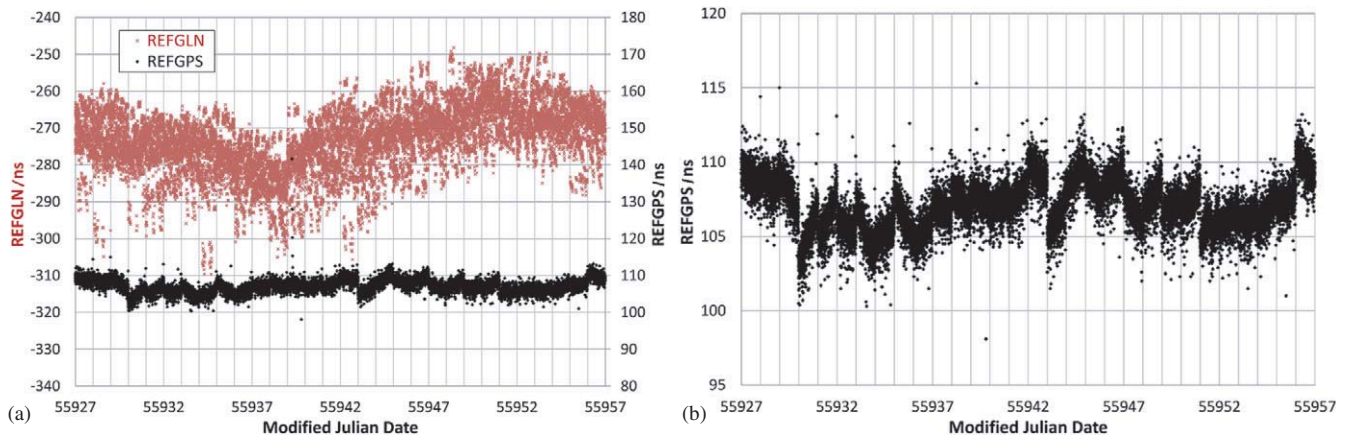


Figure 3. GPS and GLONASS REFSYS corrected with ESOC precise orbits and clocks for the Brussels station BRUX (a). Zoom over the BRUX REFGLN solution corrected with ESOC precise orbits and clocks (b). Only observations with elevation greater than 8° are reported.

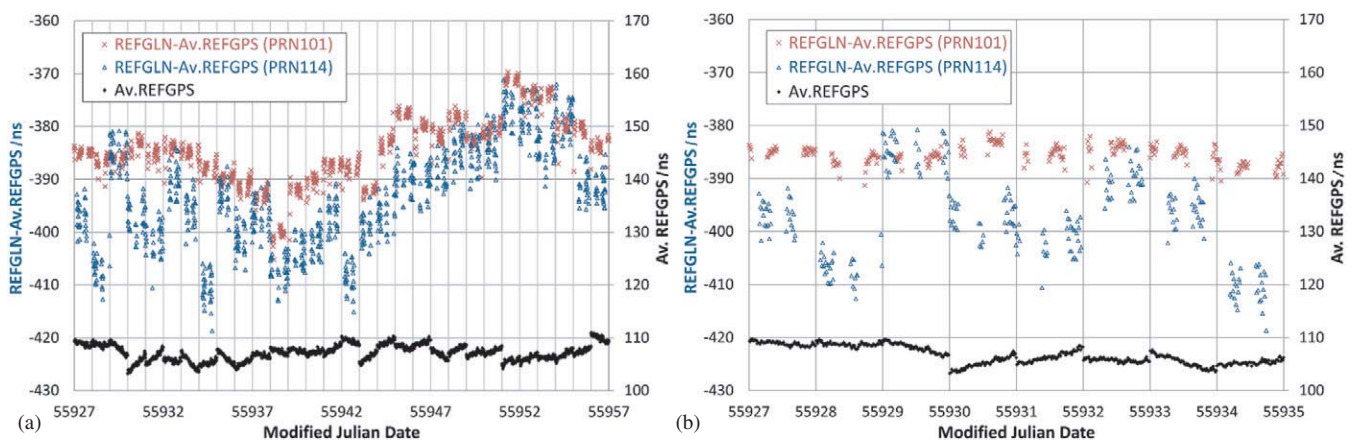


Figure 4. Comparison between the REFGLN obtained for two particular satellites and the AV REFGLN clock solution, both obtained using ESOC precise orbits and clocks for BRUX. (a) During a one-month period, (b) zoom over the first week of the period.

products. Once CGGTTS solutions are corrected, the comparison between REFGLN and REFGPS (figure 3(a)), shows two important characteristics: firstly, there are some daily discontinuities in both solutions. They are highlighted by REFGLN data (figures 3(b) and 4) whereas they are not visible on REFGPS data because their magnitude is lower than the noise of the REFGLN clock solution. These discontinuities are due to the reference clock used by the ESOC which can change from day to day; as the reference disappears when computing the time transfer link, these discontinuities and other variations due to changes of the references do not affect the time transfer results. Secondly, one can observe some variations between the GPS solution and the GLONASS solution, while these two represent the comparison between the same local clock and a common ESOC reference. These variations are due to the fact that the day boundary discontinuities in the GLONASS solution are not the same as those in the GPS solution. This difference finds its origin in the computation approach used by ESOC for clocks: ESOC operates daily computations, and for each day they determine a bias for each receiver-satellite pair. As only differences between receiver and satellite clock parameters appear, it is only possible to solve for the GLONASS clock parameters in a relative sense. ESOC therefore constrains one bias for one given station, but this

bias can change from day to day so that all biases change accordingly. This is illustrated in figure 4(a) which shows the differences between the REFGLN solutions of two particular GLONASS satellites and the AV GPS solution for the station BRUX. We clearly see that the bias between the GLONASS satellites 101 and 114 varies from day to day. This has no physical origin, as the receiver and antenna biases should be constant from day to day, it is only due to the computation of satellite clocks and receiver-satellite-dependent biases, which is carried out daily. Note that the ESOC improved their processing in December 2012 by fixing one bias, rather than constraining it. This gives a better stability to the biases while they are still determined on a daily basis. In order to be consistent with the clock products used, which are computed on a daily and satellite basis, it was decided to compute the IFBs for each satellite and for each day separately from the CGGTTS results corrected with ESOC products.

3.3. Determination of IFBs

The procedure we propose takes into consideration the discontinuities of the ESOC clock products (shown previously, figures 3–4) in the determination of the IFBs. It consists in calculating, for each day (d), the offset between the REFGLN and REFGPS corrected with precise satellites orbits and clocks.

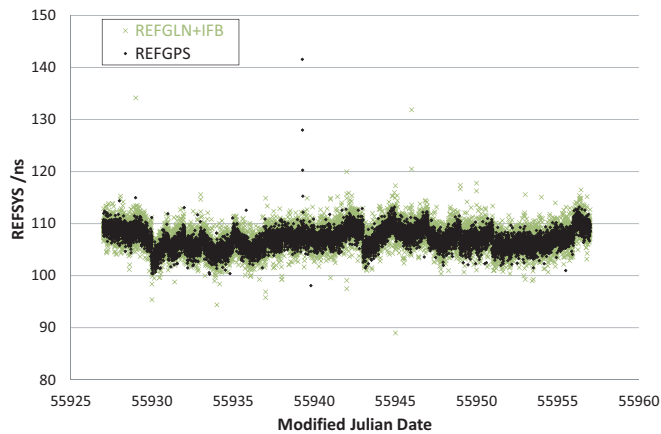


Figure 5. BRUX REFGLN values corrected with precise orbits and clocks and with IFBs (crosses) compared with the REFGPS values (dots).

In order to use a REFGPS reference as stable as possible, it has been decided to use AV GPS data (Av.REFGPS) obtained with the elevation-dependent weighting procedure used for TAI calculation [6]. $w(\text{sat}, t)$ is the weight of the observation which corresponds to $\sin^2(\text{elevation})$.

In order to ensure removal of outliers from IFB evaluation, the differences between $\text{REFGLN}(\text{sat}, t)$ and $\text{Av.REFGPS}(t)$ are filtered with the median absolute deviation technique, which is a robust statistical tool with low impact of outliers (see details in [17]). From this we compute the daily IFB of each satellite as

$$\text{IFB}(\text{sat}, d) = \frac{\sum_{t=1}^n w(\text{sat}, t) (\text{REFGLN}(\text{sat}, t) - \text{Av.REFGPS}(t))}{\sum_{t=1}^n w(\text{sat}, t)}, \quad (4)$$

where n is the number of 13 min observation tracks of this satellite during the day. The uncertainty of the biases so determined for one satellite is a function of the number of observations of this satellite and of the noise of the GPS AV solution. Typically, daily IFBs determined in our process have a 1-sigma uncertainty of about 2 ns.

The IFBs are thereafter removed from the REFGLN:

$$\text{REFGLN}_{\text{corrected}}(\text{sat}, t) = \text{REFGLN}(t) - \text{IFB}(\text{sat}, d). \quad (5)$$

In figure 5, the REFGLN clock solutions corrected with precise orbits, clocks and IFBs are reported (crosses) for each GLONASS satellite with an elevation higher than 8° . REFGPS values (dots) are also shown as comparative results. One can observe that correcting the IFBs daily for each satellite gives REFGLN values which have a dispersion slightly larger than the REFGPS values, but the GLONASS dispersion was reduced by a factor of two between figure 3(a) (i.e. before the IFBs' correction) and figure 5 (i.e. after the IFBs' correction).

4. IFB correction results in the frame of GPS+GLONASS AV combination

4.1. Effect of IFB correction on GLONASS time links

Once the GLONASS REFGLN results have been corrected for the IFB using (4), they can be combined in an AV solution, either using only GLONASS data or using GPS and GLONASS together (these solutions are obtained using a weighted average with the same weighting scheme as described previously). This section presents the comparison between the solutions obtained with these different approaches for different time links based on different receiver types and baseline lengths. Receivers used in this analysis are those reported in table 1. To compute time links, GPS and GLONASS results obtained with R2CGGTTS have been corrected with precise ephemeris and clocks using ESOC products, and corrected for IFBs as explained in the previous section. For completeness, both types of time links (all-in-view and common-view) are reported below. Table 2 presents the standard deviation of residuals with respect to a Vondrak smoothing with an ε coefficient of 10^5 for the different time transfer solutions: (1) obtained with GPS data only ('GPS'), (2) obtained with GLONASS data only ('GLN'), (3) obtained with GLONASS data only corrected IFB ('GLN (IFB)'), and (4) obtained using a mix of GPS data and GLONASS data corrected with IFBs ('GPS+GLN (IFB)'). These standard deviations are expressed in nanoseconds. The column '100 × Gain IFB' corresponds to the improvement percentage between the GLONASS solutions without and with the IFB correction.

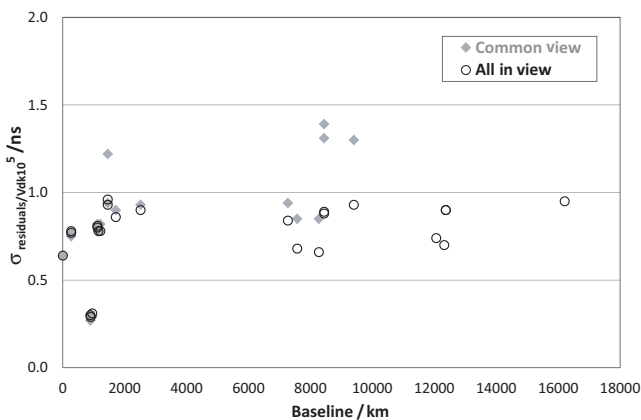
For all time links investigated an obvious improvement can be observed when correcting the results for the IFBs. The improvement ranges from 35% to 90% for the links computed using AV, and from 9% to 90% when they are computed using CV. Of course the standard deviation of the residuals before correcting for the IFBs depends on the IFBs' magnitude for the link considered, and the improvement is more significant for the links with the largest biases. The average improvement is of about 60%, i.e. the residuals are 2.5 times smaller after the IFB correction. Moreover, the GLONASS solutions after removing IFBs have a noise level which is of the same order of magnitude as that of the GPS solutions. As a consequence, when it is combined with the GPS data, the noise of the combined solution becomes equal to or smaller than the noise of the GPS-only solution in the majority of the links.

4.2. AV or CV

Figure 6 presents for the different time links the standard deviations of the CV and AV solutions obtained with combined GPS + GLN (IFB). One advantage of combining GPS and GLONASS in CV would be the increase in number of observations, especially for long baselines where the number of satellites in common visibility is rather small. However, the CV for long baselines does not provide good results even when adding GLONASS data to the GPS ones. We therefore recommend the use of AV also when combining GPS and GLONASS.

Table 2. Time links residuals obtained (compared with Vondrak smoothing with a parameter $\varepsilon = 10^5$). Values are expressed in nanoseconds. Empty fields correspond to long baseline CV for which no CV observations are available.

Time link	All-in-view					Common-view					Baseline/ km
	GPS	GLN	GLN (IFB)	GPS+GLN (IFB)	100× Gain IFB	GPS	GLN	GLN (IFB)	GPS+GLN (IFB)	100× Gain IFB	
AO_4–BP1B	0.80	6.05	0.92	0.80	85	0.83	5.70	0.89	0.81	84	1120
BP1C–BP1B	0.64	2.34	1.16	0.64	50	0.68	2.00	0.95	0.64	53	0
IP02–BP1B	1.29	1.80	1.17	0.93	35	1.37	1.32	1.20	0.94	9	1450
VN3P–BP1B	0.89	3.74	1.28	0.89	66	1.38	2.23	1.62	1.31	27	8440
VN3P–SYDN	0.84	4.40	1.21	0.84	73	0.94	4.39	1.29	0.94	71	7270
AO_4–VN3P	0.68	5.95	1.17	0.68	80	0.90	7.34	1.22	0.85	83	7570
BP1C–VN3P	0.89	3.94	1.30	0.88	67	1.69	2.79	1.78	1.39	36	8440
IP02–VN3P	1.30	3.80	1.39	0.93	63	1.66	2.17	1.75	1.30	19	9400
AO_4–IP02	1.24	6.09	0.94	0.90	85	1.34	6.11	0.91	0.93	85	2510
BP1C–IP02	1.35	2.67	1.31	0.96	51	1.41	1.87	1.33	1.22	29	1450
BP1C–AO_4	0.78	6.58	1.26	0.81	81	0.82	7.40	1.26	0.82	83	1120
AO_4–SYDN	0.73	6.79	0.89	0.74	87						12060
BP1C–SYDN	0.91	3.70	1.31	0.90	65						12370
IP02–SYDN	1.31	3.25	1.22	0.95	62						16210
SYDN–BP1B	0.91	3.57	1.22	0.90	66						12370
AO_4–BRUX	0.31	5.21	0.54	0.29	90	0.33	4.63	0.49	0.30	89	900
IP02–BRUX	1.23	2.32	0.88	0.86	62	1.32	1.85	0.89	0.90	52	1710
VN3P–BRUX	0.68	3.30	0.92	0.66	72	0.91	1.78	1.18	0.85	34	8270
BP1B–BRUX	0.77	2.14	0.89	0.77	58	0.79	1.70	0.86	0.75	49	270
BP1C–BRUX	0.78	2.41	1.19	0.78	51	0.77	2.36	0.95	0.77	60	270
SYDN–BRUX	0.73	3.56	0.88	0.70	75						12320
SPT0–BP1B	0.77	1.77	0.91	0.78	49	0.84	1.31	0.95	0.82	27	1210
ONSA–BP1B	0.80	2.45	0.90	0.78	63	0.81	1.76	0.92	0.78	48	1150
SPT0–BRUX	0.37	1.84	0.59	0.31	68	0.36	1.5	0.5	0.29	67	950
ONSA–BRUX	0.35	2.99	0.56	0.30	81	0.34	3.24	0.48	0.27	85	890

**Figure 6.** Dispersion of GPS + GLN (IFB) combination in CV (grey) and AV (black) as a function of the baseline of the time link. Y-axis represents the standard deviation of residuals to Vondrak 10^5 smoothed curve (values extracted from table 2).

Two examples of time links are presented in figures 7 and 8. In each case we present the solutions obtained in AV from GPS only, GLONASS-only, GLONASS-only corrected for IFBs and GPS combined with GLONASS corrected for IFBs. In these figures, the improvement brought when correcting for IFBs appears clear and the comparison of the GPS-only solutions with the combined GPS + GLN (IFB) solutions gives differences of only a few picoseconds.

After observing the improvements brought by correcting for IFBs on the noise of the time links, another important parameter to observe is the incidence of correcting for IFBs

on the modified Allan deviation, to compare efficiency of the use of AV GPS and combined AV GPS+GLONASS at all averaging times. Figures 9(a) and (b) present the stabilities obtained for the two links presented before. It appears clearly that the addition of GLONASS data in the time link provides a stability very similar to the one obtained from GPS-only. This result confirms the conclusions of Defraigne and Baire [14] who introduced GLONASS data in time transfer using precise point positioning, i.e. a combination of code and carrier phases.

4.3. IFB obtained for various receivers

The physical origin of the IFBs is a frequency dependence of the satellite and receiver hardware delays. This implies that the IFBs of a given receiver–satellite pair should be constant over time. However, we have shown in section 3.2 that this is not the case, as we observed day-to-day variations of the IFBs of a given receiver and furthermore we could see that these variations are not exactly the same for all the satellites. As explained before, this is a consequence of the procedure used by ESOC to compute satellite clock products. The IFBs for a given satellite can therefore be written as the sum of a constant bias of physical origin, $\delta_{\text{rec}}(f)$, with f the frequency emitted by the satellite, plus a term varying each day due to the daily computation by ESOC, $\delta(\text{sat}, \text{day})$:

$$\text{IFB}_{\text{rec}}(\text{sat}, \text{day}) = \delta_{\text{rec}}(f) + \delta(\text{sat}, \text{day}). \quad (6)$$

To verify the existence of this constant satellite–receiver bias, we compared the variations of $\text{IFB}_{\text{rec}}(\text{sat}, \text{day})$ over the 30 days

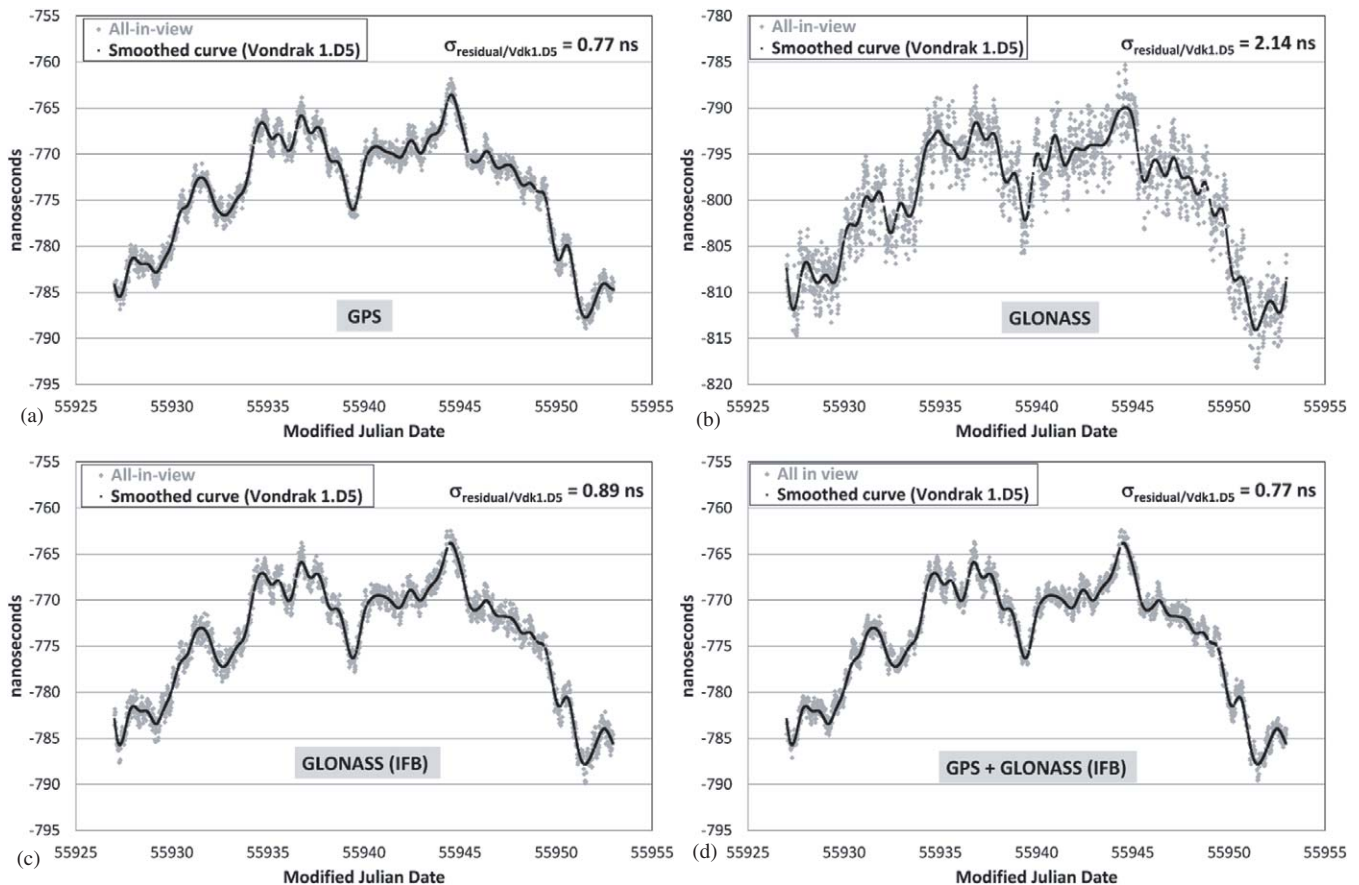


Figure 7. AV time links results for BP1B–BRUX: GPS (a), GLONASS (b), GLONASS (IFB) (c) and combination GPS + GLONASS (IFB) (d).

for a given satellite and several receivers. If these variations are the same for all the receivers, this means that they are only due to the ESOC products, not to an instability of receiver hardware delays. The IFB variations are then only due to the second term in the expression here above, and the first term is therefore constant. Figure 10 presents the variations from day to day of the IFBs of two particular satellites (PRN 101 and PRN 108) for the different receivers. We can confirm that for a given satellite, the variation of the IFB is the same for all the receivers. The differences between two curves (after removing a constant bias) do not exceed 4 ns peak to peak, which is in agreement with the 2 ns uncertainties on the computed IFBs (see section 3.3). Note that the station AO_4 is the only one showing larger variations, up to 8.5 ns peak to peak, which can currently not be explained. Note also that a part of the variations of $\delta(\text{sat}, \text{day})$ is due to a variation of the mean ESOC bias, which explains why some patterns are observed both for PRN 101 and PRN 108.

We can also look at the mean IFB for each satellite–receiver pair over one month. Using equation (6) here and considering $\delta_{\text{rec}}(f)$ as constant during the month, we obtain

$$\langle \text{IFB}_{\text{rec}}(\text{sat}) \rangle = \delta_{\text{rec}}(f) + \frac{1}{N} \sum_{d=1}^N \delta(\text{sat}, d). \quad (7)$$

The results are illustrated in figure 11 for the station BRUX. It can be seen that two satellites on the same frequency channel

have different biases. This is a consequence of the ESOC processing technique in which some biases are estimated for each satellite rather than for each frequency, which justifies that we have to determine the IFBs on a satellite basis rather than on a frequency basis.

In order to look for possible correlation between the receiver type and the IFBs, it is necessary to fix one receiver as the reference, and to compare the mean IFBs of the other receivers to the mean IFBs of the reference receiver. This allows removal from the IFBs of the variable part $\langle \delta(\text{sat}, \text{day}) \rangle$ coming from the ESOC products and to keep only the receiver hardware delays. We present therefore in figure 12, the differences between the mean IFB of each satellite–receiver pair and the corresponding mean IFB of BP1B; the reference receiver is therefore a TTS-3/4. The mean IFBs have been computed as the average over the period indicated in table 1 for each receiver. A first observation concerns the receiver TTS-3/4 in AO_4 which shows a very important frequency dependence of its IFBs, with increasing biases for increasing frequency (except for the frequency -7). This behaviour clearly does not exist for any of the two other TTS-3/4 receivers (BP1B and IP02). A second observation concerns the two receivers JPS E_GGD (ONSA and SYDN) which have clearly the same frequency dependence of IFBs. An obvious correlation can also be seen for the three Septentrio PolaRx3eTR receivers (BRUX, BP1C, VN3P): their biases are spread over a shorter range of values (within 10 ns),

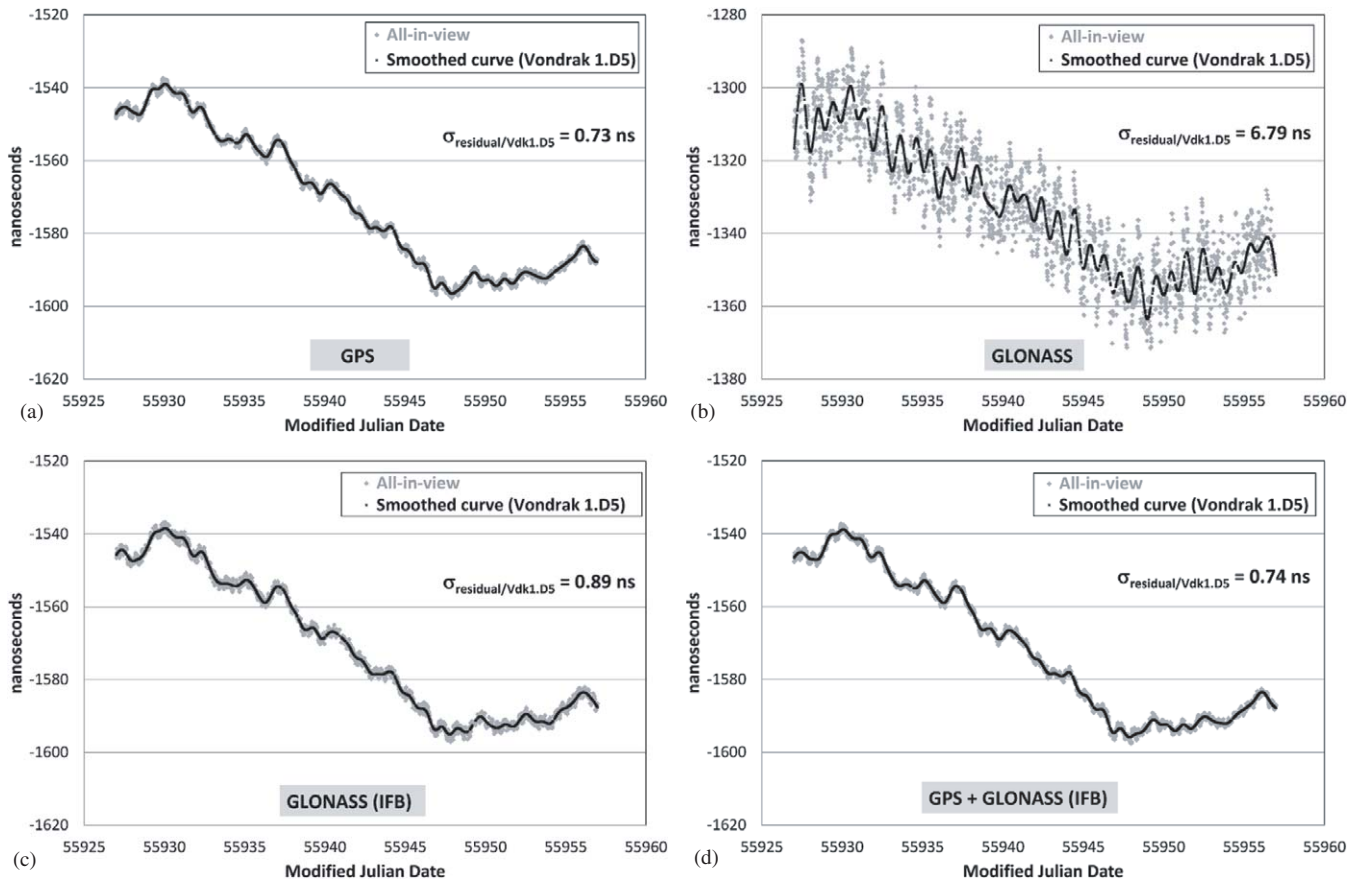


Figure 8. AV time links results for SYDN-AO.4: GPS (a), GLONASS (b), GLONASS (IFB) (c) and the combination GPS + GLONASS (IFB) (d).

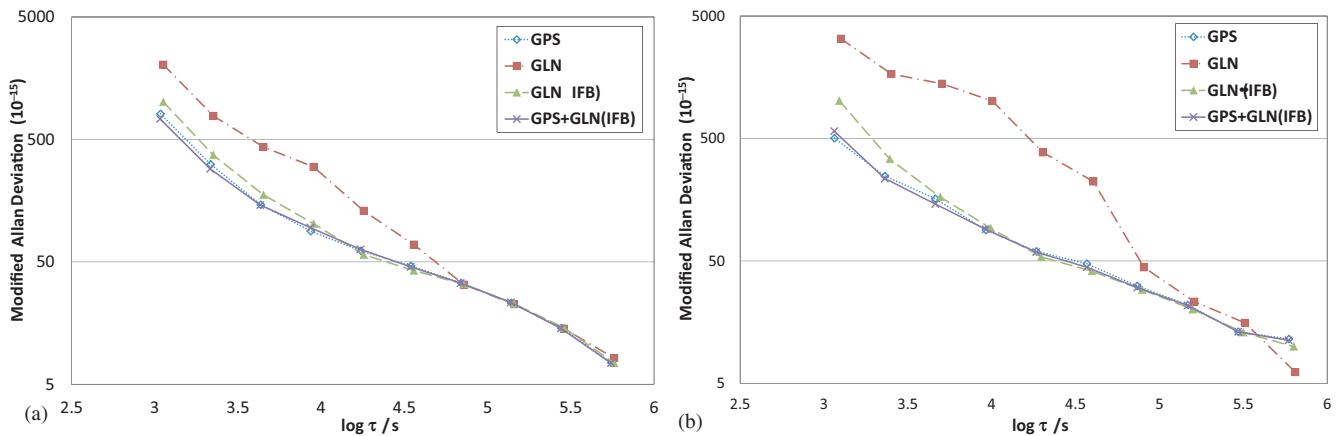


Figure 9. Modified Allan deviation of AV time links BP1B-BRUX (a) and AO.4-SYDN (b).

they all show the same dependence on the frequency, but this dependence is not linear (or quasi-linear) as for the JPS E_GGD, but that does not exclude a linear dependence which would be similar to that for the BP1B receiver, and which would be superimposed on the variations observed in figure 12. Note that because R2CGGTTS does not correct GLONASS data for the P1C1 and P2C2 biases which are linked to each satellite when C1 and/or C2 is used to make the combination (this has been the case for BP1C, BRUX, VN3P), these biases appear in the calculated IFBs. This could explain discrepancies in the

bias value between two satellites using the same frequency, and the non-quasi-linear relation between the frequency and the IFBs for these three receivers.

5. Conclusion

The goal of this study was to develop the necessary tools for using ionosphere-free codes of GLONASS as is already carried out for GPS in the *Circular T* calculation at the BIPM. With that aim, an upgrade of the R2CGGTTS software is

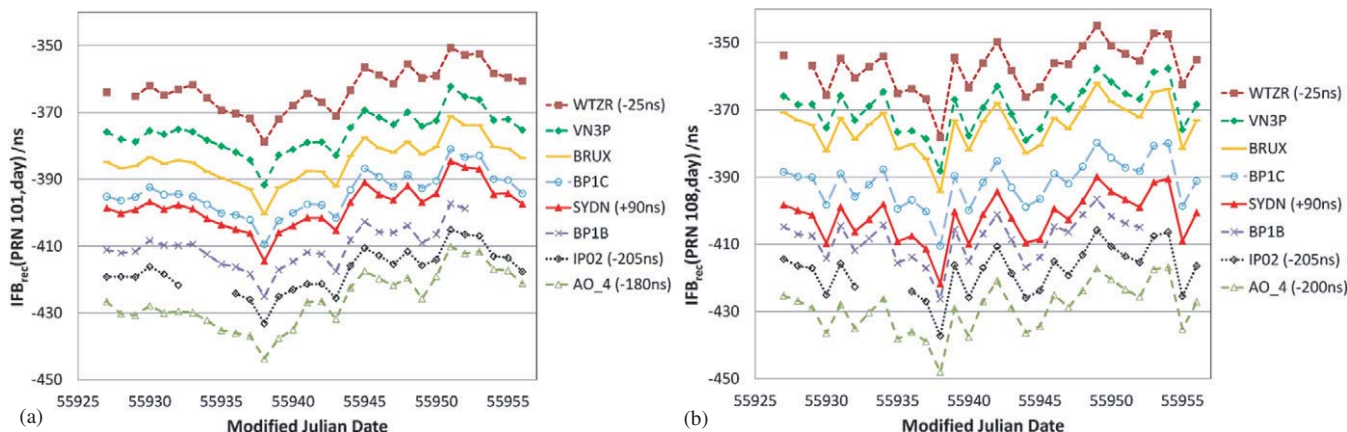


Figure 10. Variation of the daily IFB of two GLONASS satellites (PRN101 (left) and PRN108 (right)) for several different receivers between MJD 55927 and 55957. WTZR, SYDN, IP02 and AO_4 PRN101 and PRN108 biases have been corrected by, respectively, -25 ns, $+90$ ns, -205 ns, -180 ns and -200 ns to improve the visibility.

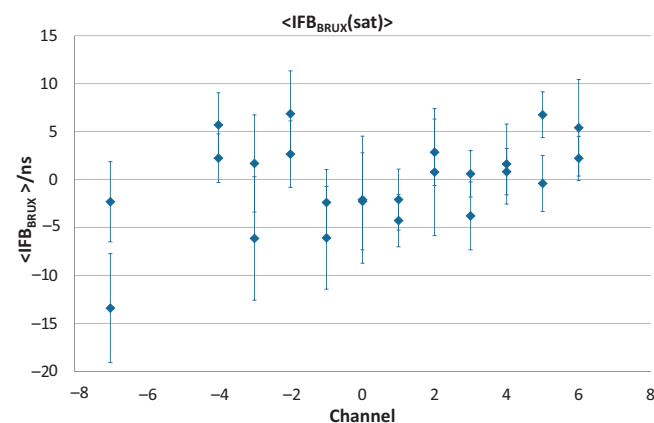


Figure 11. Mean IFBs determined for BRUX, for each satellite over 30 days (between MJD 55927 and 55957) for station BRUX. Error bars represent the standard deviation over the interval.

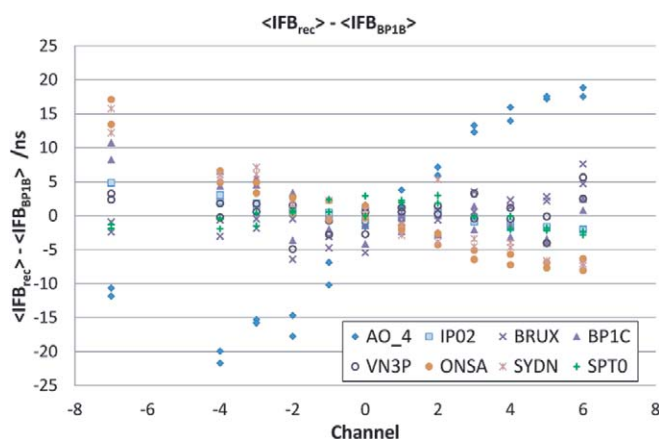


Figure 12. Differences between the mean IFB of each satellite and receiver and the corresponding mean IFB of BP1B (list of receivers given in table 1).

proposed: version 5 enables the analysis of both GPS and GLONASS data based on the dual-frequency combination of code measurements on the two frequencies $L1$ and $L2$. The combination of GPS and GLONASS in all-in-view was then

studied. Due to the specificity of GLONASS satellites to emit on different frequency channels, GLONASS clock solutions must be corrected for frequency-dependent receiver delays (IFBs for inter-frequency biases) before any combination in a global solution. These delays have been computed with respect to the REFGPS all-in-view solution for a set of nine stations. Differences between IFBs for the same station have been shown to be as large as 25 ns. As only ESOC clock products are providing GPS and GLONASS clocks with respect to the same reference, which is mandatory for the combination of both constellations in one all-in-view solution, and because these satellite clock products have been computed on a daily basis, and with one daily bias for each satellite, we are currently obliged to determine the IFBs daily and for each satellite, while physically these IFBs should be constant with time. Our study has shown that correcting the GLONASS solution for IFBs reduces strongly the noise of the GLONASS solution, with a significant noise reduction (from 35% to 90%) for the time links investigated.

From the comparison between CV and AV results, it was concluded that even when increasing the number of observations in CV thanks to the combination of the two constellations, the AV remains superior to the CV solution in terms of noise and short term stability, especially for long baselines.

GPS and GLONASS ionosphere-free combinations in all-in-view solutions were also compared to the GPS-only all-in-view solutions. For some links where one of the receivers has a quite large GPS code noise level, the noise of the combined solution is better than the noise of the GPS-only solution. For the other time links, the noise level of both solutions is equivalent. For all the links investigated, the statistical uncertainty of the GPS + GLONASS (IFB) AV combination was smaller than 0.95 ns.

The IFBs of different receivers have also been compared, and the conclusion was that, except for one particular receiver (AO_4), receivers coming from the same manufacturer and same model have the same relation between the frequency and the IFBs.

A further step in this use of GLONASS data will be to use the biases computed as by-products of the GLONASS

satellite clocks in the ESOC process, when these biases become available. This should allow one to remove the day-to-day variations of the IFBs computed in our approach, and to keep in them only a receiver bias which could therefore be fixed as a constant over one given period (one month for example, i.e. the data batch length used for the BIPM *Circular T* computation). When having these biases at our disposal, it will make sense to organize receiver calibration for each of the GLONASS frequency channels in parallel to the calibration of the GPS channels. Then it will no longer be necessary to determine the IFBs as shown in this paper; we will fix the biases to the values obtained from calibration data and from the ESOC biases, as currently carried out for GPS hardware delays.

Acknowledgments

The authors thank the laboratories for providing data for TAI and the IGS, which provided most of the data used in this study. Tim Springer and the ESOC are also thanked for helpful discussions and for making available satellite orbits and clocks. The authors also thank Laurent Tisserand who contributed in supplying BIPM RINEX and CCGTTS files.

References

- [1] Allan D W and Weiss M 1980 Accurate time and frequency transfer during common-view of a GPS satellite *Proc. IEEE Frequency Control. Symposium (Philadelphia, PA)* pp 334–56
- [2] Allan D W and Thomas C 1994 Technical directives for standardization of GPS time receiver software *Metrologia* **31** 69–79
- [3] Azoubib J and Lewandowski W 1998 CCGTTS GPS/GLONASS data format Version 02 *7th CCGTTS Meeting (Reston, VA)*
- [4] Defraigne P and Petit G 2003 Time transfer to TAI using geodetic receivers *Metrologia* **40** 184–8
- [5] Petit G and Jiang Z 2008 GPS All in view time transfer for TAI computation *Metrologia* **45** 35–45
- [6] Defraigne P, Petit G and Bruyninx C 2001 Use of geodetic receivers for TAI *33rd Annual Precise Time and Time Interval (Long Beach, CA)*
- [7] Petit G and Jiang Z 2004 Stability and accuracy of GPS P3 time links *Proc. 18th European Frequency and Time Forum (Guildford, UK)*
- [8] Lewandowski W and Jiang Z 2009 Use of GLONASS at the BIPM *41st Annual Precise Time and Time Interval (PTTI) Meeting (Santa Ana Pueblo, NM)*
- [9] Wolf P and Petit G 1999 Use of IGS ionosphere products in TAI *Proc. 31st Annual Precise Time and Time Interval Meeting (Dana Point, CA)* pp 419–29
- [10] Roosbeek F, Defraigne P and Bruyninx C 2001 Time transfer experiments using GLONASS P-code measurements from RINEX files *GPS Solutions* **5** 51–62
- [11] Nawrocki J *et al* 2006 An experiment of GPS+GLONASS common-view time transfer using new multi-system receivers *Proc. European Frequency and Time Forum* pp 904–9
- [12] BIPM 2011 *BIPM Annual Report on Time Activities* vol 6 http://www.bipm.org/utls/en/pdf/time_ann_rep/Time_annual_report_2011.pdf
- [13] Matsakis D 2007 The Timing Group Delay (TGD) correction and GPS timing biases *Proc. 63rd Annual Meeting of the Institute of Navigation (Cambridge, MA)* pp 419–29
- [14] Defraigne P, Baire Q and Harmegnies A 2010 Time and frequency transfer combining GLONASS and GPS data *42nd Annual Precise Time and Time Interval Meeting (Reston, VA)* pp 263–74
- [15] Report of the ICG Working Group A 2007 *Second Meeting of the International Committee on Global Navigation Satellite Systems (ICG) (Bangalore, India)*
- [16] Jiang Z and Lewandowski W 2012 Use of GLONASS for UTC time transfer *Metrologia* **49** 57–61
- [17] Harmegnies A, Panfilo G and Arias E F 2009 Detection of outliers in TWSTFT data used in TAI *41st Annual Precise Time and Time Interval Meeting (Santa Ana Pueblo, NM)* pp 421–32